Surface Film Adsorption and Lubricity of Soybean Oil In-Water Emulsion and Triblock Copolymer Aqueous Solution: A Comparative Study

Reza Taheri, Buyung Kosasih *, Hongtao Zhu and Anh Kiet Tieu

School of Mechanical, Materials and Mechatronics Engineering, University of Wollongong, Wollongong 2522, NSW, Australia; rt795@uow.edu.au (R.T.); hongtao@uow.edu.au (H.Z.); ktieu@uow.edu.au (A.K.T.)
* Correspondence: buyung@uow.edu.au

Abstract: This paper investigates the surface film adsorption and lubricity of two different types of potential environmentally friendly cold metal forming lubricants: soybean vegetable oil in water *VO/W* emulsions and triblock copolymer aqueous solutions. The lubricants have different visual appearance, surface film adsorption characteristic, lubricity and surface cleaning behaviour. The effects of concentration, temperature and emulsification ultrasonic energy (for *VO/W* emulsion) are studied. The result shows that the soybean *VO/W* emulsions have stronger adsorption, superior lubricity and anti-wear property compared to the copolymer solutions. The effect of temperature is investigated at 30 °C and 65 °C which are below and above cloud point of the aqueous copolymer solutions. Both lubricants show improved friction and anti-wear property at 65 °C. However, tenacious residual film remained on the discs surface after surface cleaning indicates lower cleanability of the soybean *VO/W* emulsions compared to the copolymer solutions, postulating the need for extra post-processing cleaning operations after cold forming process with *VO/W* emulsion lubricant.

Keywords: adsorption; environmentally friendly lubricant; lubricity; vegetable oil in water emulsion; triblock copolymer solution

1. Introduction

Lubricating oils have evolved rapidly from the conventional mineral oil based lubricants to synthetic oils and aqueous solutions to the extent that more than 10,000 different lubricants are currently in use [1]. However, significant health hazard and increased cost of mineral oils have driven a global shift to promote green alternatives as the potential substitutes. Water based lubricants are low cost environmentally-friendly substitutes for mineral oil based lubricants. Two types of water based lubricants namely oil in water *O/W* emulsions [2–6] and aqueous copolymer solutions [7–10] have been studied.

Biodegradable, non-toxic, and environmentally friendly vegetable oil [11] with superior tribological properties than conventional mineral oil [12–14] is a potential mineral oil substitute. When used as vegetable oil in water emulsion (referred to as *VO/W* emulsion in this work), the heat convection property of the aqueous phase complements the friction reducing property of the oil phase [2]. Additionally, the study of the lubricity of different vegetable oils suggests that a small concentration of vegetable oil (1%–5% content) in a *VO/W* emulsion [6] has comparable lubricity to conventional oil based lubricants [15–17]. This makes vegetable oil in water emulsion a cost effective green and renewable lubricant with low oil consumption, in accordance with the minimum quantity lubricant *MQL* strategy [18,19]. Aqueous triblock copolymer solutions are another class of low cost aqueous alternatives, possessing comparable tribological performance to conventional lubricants and excellent surface cleanability [8,20,21].

Oil in water *O/W* emulsion has been used in cold rolling of steel strips in mostly mixed film lubrication regime and studied extensively [3,4,22–24]. The film formation mechanism of *O/W* emulsion in the inlet zone of the rolling pairs is condition dependent (i.e., on the rolling speed, the droplet size, concentration etc.), and can generally be explained by plate-out phenomenon, i.e., oil droplets entrainment into the contact zone of the rolling pairs or oil pool formation between the rolling pairs [4,22–24]. Nakanishi et al. [23] shows that plate-out oil pool volume increases with oil concentration and droplet size. At lower sliding speed, the larger droplets play a dominant role in the formation of the oil pool while the finer droplets' role is dominant at higher sliding speed [22]. At high reduction ratio and low speed when there are more asperity contacts and the mixed film regime is closer to boundary film regime, *O/W* emulsions are as effective as the neat oil [4], attributed to the formation of oily films between rubbing pairs. With this background, the motivation of this work is to study the substitution of mineral oil component of the emulsion with vegetable oil as in *VO/W* emulsion.

Most vegetable oils are mainly triglycerides composed of triesters of glycerol and fatty acid chains [16,25]. Glycerol ($C_3H_8O_3$) is the backbone attached to the fatty acid chains through the $C-O$ ester bonds. Fatty acids are aliphatic carboxylic acid chains with single and double bonded carbon atoms [11,26]. Triglyceride absorbs to the metal surface through the polar glycerol head while the nonpolar hydrocarbon chain of fatty acids extends out forming mono-/multi-molecular layer [27]. It is also known that the triglycerides structure (i.e., fatty acid composition, chain length, and unsaturations) influences the lubricity of vegetable oil based lubricants [14,16,28]. The polar nature of triglycerides increases the monolayer film adsorption propensity thus making vegetable oils suitable for boundary regime lubrication [16]. However, thermo-oxidative instability due to the presence of bis-allylic protons has limited the use of polyunsaturated vegetable oil based lubricants [25,29].

Triblock copolymers are classified as normal $PEO_mPPO_nPEO_m$ with two hydrophilic PEO *poly-(ethylene oxide)* end blocks and one hydrophobic PPO *poly-(propylene oxide)* middle block and reverse $PPO_nPEO_mPPO_n$ with two PPO end blocks and one PEO middle block. The two copolymers have different behaviour in aqueous environment [30]. Copolymers are interfacially active and adsorb on the surface via either the hydrophobic PPO or the hydrophilic PEO blocks [31]. Adsorption of normal copolymers on metal surface is postulated through the anchoring of the PPO blocks through hydrophobic interactions with the surface, leaving the PEO blocks extended out in the solution, forming a steric bulky 'brush-like' PEO layer [7,32]. Similarly, adsorption of reverse copolymers is through the PPO blocks albeit with different mechanism [33,34]. At below cloud point and below critical micellisation concentration *CMC*, adsorbed copolymers mass and thickness increase with concentration [35,36] while the friction coefficient decreases depending on the PPO molar mass [37]. Previous studies also indicate that micellisation plays a significant role in both the adsorbed layer and lubricity [34,38]. In the authors' previous study [34], the adsorbed mass and lubricity of four triblock copolymers (commercially known as L62, L64, 17R2, and 17R4) were investigated, where the increase in adsorbed mass and the significant improvements in lubricity from 8% to 18% concentration were attributed to the micelles-dominated adsorbed layer.

The amount and the tenacity of the adsorbed film and its friction reducing property are important factors in the lubricity of lubricants. Additionally, in metal forming processes the ease of surface cleaning from the film residue and the reactive lubricants is also another important requirement [39]. It is thus necessary to consider the lubricant residuals left on the surface after the process. This work, following the authors' previous works [7,8,34], compares the lubrication performance of *VO/W* emulsions and copolymer aqueous solutions through ball-on-disc tests, and via surface mass adsorption measurements and microscopy analyses to study their interfacial behaviour. Concentrations reported herein are volume percentage vol% unless otherwise indicated.

2. Experiments

Materials: 18% aqueous solutions of normal copolymer L64 ($PEO_{13}PPO_{30}PEO_{13}$) (Sigma Aldrich, Castle Hill, Australia) and reverse copolymer 17R4 ($PPO_{14}PEO_{24}PPO_{14}$) (BASF, Southbank, Australia)

were prepared. Additive-free *VO/W* emulsions from polyunsaturated soybean oil (SB) (Cargill, Kooragang, Australia) with 23.4% oleic (C18:1), 56.1% linoleic (C18:2), 8.5% linolenic (C18:3), and 15% stearic (C18:0) and palmitic (C16:0) acids [40] were prepared at 1% and 2% concentration via ultrasonication using *Sonoplus HD3200* ultrasonic mixer. As the control parameter, the *FTIR* spectra of the soybean oil is shown below in Figure 1 and along with the copolymers *FTIR* spectra is summarised in Table 1. 300 mL of emulsions were prepared at the controlled ultrasonication energy of 5 kJ and 10 kJ, with similar *FTIR* spectra to that of the neat soybean oil. All samples were used as received without purification and prepared with *Milli-Q* water at least 24 h prior to tests. Figure 2 shows the differences in the samples' appearance. Stable dispersion of the *VO/W* emulsions without additional dispersant (emulsifier) was observed several weeks after the emulsification, suggesting the adequacy of the input energies (5 kJ and 10 kJ). Stainless steel SS316 discs (of 8 cm diameter and 5 mm thickness) and balls (of 4 mm diameter) were used as the tribopairs. Chromium/Gold coated 5 MHz AT-cut crystals with comparable hydrophobicity to stainless steel SS316 [34] were used as *QCM* surface model in the adsorption studies.
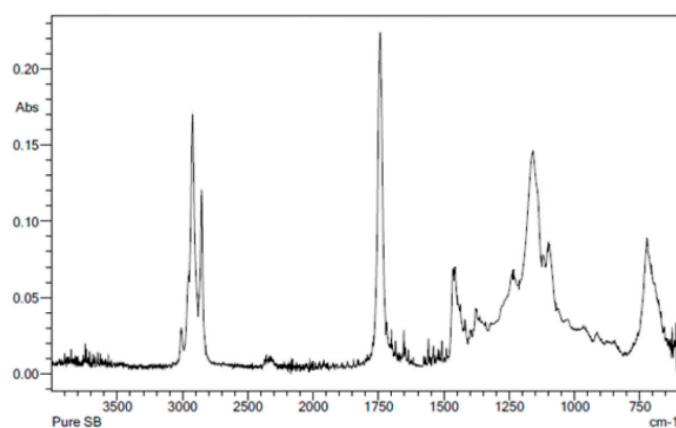

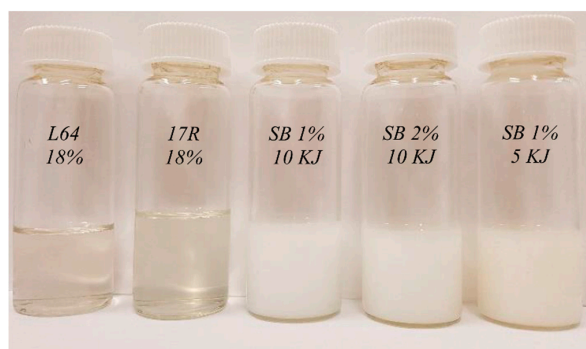**Figure 1.** Pure soybean oil *FTIR* Spectra.

Figure 2. Significant differences in samples' appearance.

Table 1. *FTIR* characterisation of pure lubricants and fresh surfaces.

#	Peak Wavenumber (cm^{-1})	Element	Functional Group	Pure Oil/Copolymers	Surface *
1	650–1000	C–H	Alkanes	All	None
2	1100–1200	C–O	Ester	All	None
3	1350–1450	CH$_2$	Methylene	17R4 & L64	None
4	1350–1450	CH$_3$	Alkyl	17R4 & L64	None
5	~1500	C=C	Alkene	Soybean Oil	None
6	~1730	C=O	Carboxylic Acid	Soybean Oil	None
7	~2860	C–H	Alkanes	All	None
8	~2950	C–H	Alkanes	All	None

* High noise on surface *FTIR* data acquisition before lubricity test.

Quartz Crystal Microbalance: Surface film adsorption behaviours of the lubricants were studied using *SRS QCM200* on 5 MHz quartz crystals. According to the *Butterworth-Van Dyke* circuit model for resistance shift (Equation (1)) and modified *Sauerbrey-Kanazawa* equation (Equation (2)) [41,42], in liquid environment and for thin, rigid, and uniform adlayer, the overall frequency shift is related to the deposited mass and resistance shift (Equation (3)). In equations, Δf_T is a function of initial frequency f_0, current frequency f, adsorbed mass Δm, angular frequency at series resonance $\omega_s = 2\pi f$, crystal properties ($\rho_q = 2.648$ g·cm^{-3}, $\mu_q = 2.947 \times 10^{11}$ g·cm^{-1}·s^{-2}), solution properties (ρ_l and η_l), resistance shift ΔR, and unperturbed resonator inductance $L = 30$ mH. Frequency shift and resistance shift were recorded during the 15 min Chromium/Gold crystal immersion in each sample (denoted as "immersion stage") and the following 10 min immersion in *Milli-Q* water (denoted as "rinsing stage"). Measurements were repeated three times and average values are reported.

$$\Delta R = \left(\frac{\omega_s L}{\pi} \right) \cdot \left(\frac{2\omega_s \rho_l \eta_l}{\rho_q \mu_q} \right)^{1/2} \tag{1}$$

$$\Delta f_T = \left(-\frac{2f_0{}^2}{\sqrt{\rho_q \mu_q}} \cdot \Delta m \right) + \left(-f_0{}^{3/2} \sqrt{\frac{\rho_l \eta_l}{\rho_q \mu_q}} \right) \tag{2}$$

$$\Delta f_T = \left(-\frac{2f_0{}^2}{\sqrt{\rho_q \mu_q}} \cdot \Delta m \right) + \left(-\frac{\Delta R}{4\pi L} \cdot \left(\frac{f_0}{f} \right)^{3/2} \right) \tag{3}$$

Fourier Transform Infrared Spectroscopy: To investigate the molecular structure of the lubricants and the residues on the worn surfaces before and after the ball-on-disc tests, *FTIR* measurements were performed on a *Shimadzu IRAffinity 1* spectrometer. Small sample drops were used and the *FTIR* generated spectrums were analysed against standard reference charts.

Ball-on-Disc: Lubricity tests were performed on a *CETR UMT2* tribometer. Both ball and disc were fully immersed in the solution for 20 min prior to each test and maintained immersed throughout the test. Similar operating conditions to Taheri et al. [34] were followed to maintain a boundary lubrication regime (80 rpm angular velocity with 20 mm radius). The average friction coefficients over 300 m sliding distance were obtained from the simultaneous measurement of normal and sliding forces using *CETR DFM-1* two axis sensor.

Scanning Electron Microscopy: Wear scar on balls and track on discs were analysed using a *JOEL JSM6490* instrument. An *Evactron Model 25* bath was used to ensure the removal of the lubricants' residues from the surface.

## 3. Results and Discussion

3.1. Surface Film Adsorption

Adsorption and desorption behaviour were characterised by means of quartz crystal microbalance (*QCM*). Figure 3 shows the interfacial adsorbed amount (per unit area, $\Delta\Gamma$) of the soybean *VO/W* emulsions. For 1% 10 kJ soybean *VO/W* emulsion (Figure 3 solid lines), stable adsorbed mass of 1.9 µg/cm^2 is reached after 15 min of immersion. In the rinsing stage (immersion in *Milli-Q* water) an apparent mass increase to 3.13 µg/cm^2 is observed. The increase in the mass sensed by *QCM* in rising stage indicates the strong polar nature of the molecules preventing the film to desorb from the surface, unless with high hydraulic current as the roll-up force [43]. A similar behaviour is also seen elsewhere [44].

The effect of ultrasonic energy input from 5 kJ to 10 kJ on the adsorbed mass of the soybean *VO/W* droplets is depicted in Figure 3a. Energy affects the droplet size and consequently the stability of the emulsion [45]. During the sample preparation, it was observed that increasing the ultrasonic input energy from 5 kJ to 10 kJ in 300 mL soybean *VO/W* emulsion reduces the average dimeter of droplets from 786 nm to 222 nm, with marginal size reduction in above 10 kJ. The greater adsorbed mass of the

5 kJ emulsion compared to the 10 kJ emulsion (Figure 3a) suggests the greater absorbance of larger droplets. Based on the mass/area ratio analysis it can be shown that for the same coverage area, larger droplets deposit more mass compared to smaller droplets. According to the *Langmuir* adsorption model, a finite number of independent adsorption sites exist on the surface [46]. For similar number of adsorption sites ($n_{5 \text{ kJ}} = n_{10 \text{ kJ}}$), the ratio of the total mass of droplet is given by

$$\frac{m_{5 \text{ kJ}}}{m_{10 \text{ kJ}}} = \frac{n_{5 \text{ kJ}}}{n_{10 \text{ kJ}}} \frac{(V_{5 \text{ kJ}}) \rho_{\text{oil droplet}}}{(V_{10 \text{ kJ}}) \rho_{\text{oil droplet}}} = \left(\frac{r_{5 \text{ kJ}}}{r_{10 \text{ kJ}}}\right)^3 \tag{4}$$

where m is the total mass on surface, n is the number of adsorption sites, and r is the radius of a droplet resting on a horizontal surface. Since the free droplet radius R is greater in the 5 kJ emulsion, $R_{5 \text{ kJ}} > R_{10 \text{ kJ}}$ and assuming that the droplets contact angle is independent of droplet size in the nanometre range [47], ($\frac{R_{5 \text{ kJ}}}{R_{10 \text{ kJ}}} \approx \frac{r_{5 \text{ kJ}}}{r_{10 \text{ kJ}}}$), it can be shown that $m_{5 \text{ kJ}} > m_{10 \text{ kJ}}$.
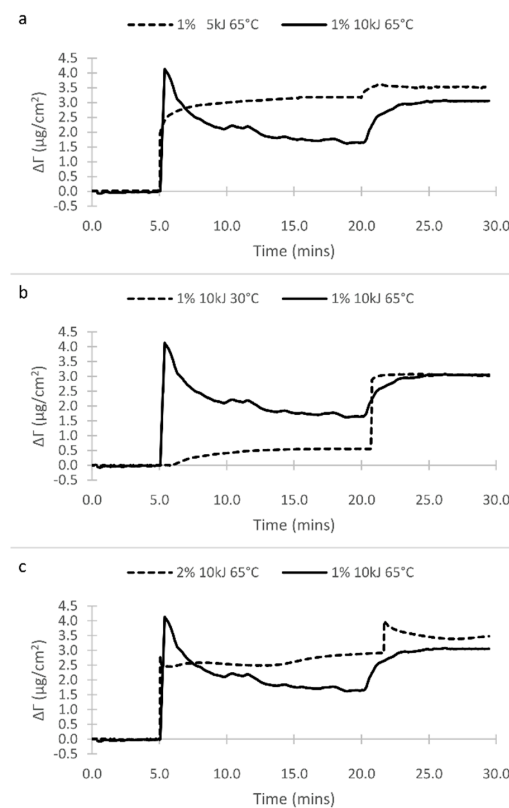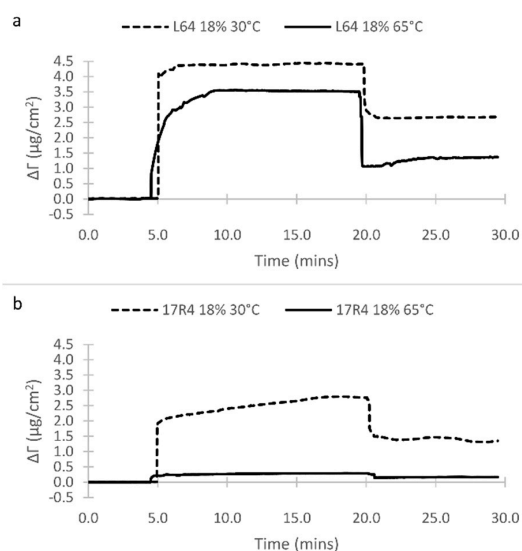

Figure 3. *QCM* adsorption trace of 1% 10 kJ soybean *VO/W* emulsion at 65 °C (solid lines) compared to (**a**) 1% 5 kJ soybean *VO/W* emulsion at 65°C, (**b**) 1% 10 kJ soybean *VO/W* emulsion at 30°C, (**c**) 2% 10 kJ soybean *VO/W* emulsion at 65°C.

A significant increase in the adsorption amount of 1% 10 kJ soybean *VO/W* emulsion from 0.54 µg/cm² to 1.9 µg/cm² with temperature increase from 30 °C to 65 °C in Figure 3b postulates the positive effect of temperature on the adsorbed mass of soybean droplets. Low adsorbed mass at the lower temperature shows low tendency of soybean fatty acids to form adhesive polar bonds with metal surface. Overall, the adsorption of soybean oil droplets on metal surface depends on factors such as the polarity of the head group, chain length, fatty acid composition, and temperature [48]. As the primary reason, polarity of the head group of soybean triglyceride molecules increases the adsorption tendency of the soybean oil droplets [48–51]. Besides, increasing the temperature (in below the transition temperature [50]) induces both the chemical reactions between the surface oxide layer and triglycerides, and chain polymerisation of unsaturated fatty acids on surface, therefore works in adsorptions favour

by providing an extra protective chemical layer on the surface [48]. Comparison between 1% and 2% *VO/W* emulsions (Figure 3c), asserts that increasing the oil concentration only slightly increases the adsorbed amount. This is possibly due to the saturation of active adsorption sites on the surface in below 2% concentration. This agrees with previous studies on vegetable oils lubricity showing that the concentration influences lubricity only below 1% [16,27].

From the copolymer solutions' *QCM* trace (Figure 4), a rapid decrease of the surface mass is seen at the rinsing stage starting point, 20 min time. Unlike the *VO/W* emulsions, this behaviour suggests the superior cleanability of copolymers solutions. Similar results are also reported elsewhere [38]. Contrary to fatty acids, which provide adhesive chemical layers on the surface through polar bonding and chemical reactions, copolymer solutions adsorb through hydrophobic interactions between the PPO blocks and the metal surface. Physically formed layers of copolymer solutions are readily rinsed due to non-polar behaviour [52]. Moreover, desorbed copolymer films have lower tendency to readsorb during the dynamic film regeneration [53]. Therefore, weaker film adsorption and lower lubricity performance of the copolymer solutions compared to the soybean *VO/W* emulsions are expected.

Figure 4. *QCM* adsorption trace of 18% aqueous solutions of (**a**) normal copolymer L64, and (**b**) reverse copolymer 17R4, at 30 °C (dash line) and 65 °C (solid line).

Contrary to soybean *VO/W* emulsions, the traces of copolymer adsorption and desorption (Figure 4) suggests a negative temperature effect on the adsorption of copolymer solutions. As pointed in previous studies and unlike the other mass detection techniques (such as *SPR*), *QCM* measures the wet mass on the crystals surface, i.e., copolymer mass coupled with water [54,55]. The interaction between the hydrophilic PEO blocks of copolymers and water at both the solid-liquid interface and bulk solution is temperature-dependant, i.e., temperature driven dehydration of PEO blocks at high temperature [56,57]. At 65 °C (above cloud point), PEO blocks dehydrate and therefore shrink, resulting in lighter adsorbed layer on interface, shown in Figure 4a,b.

Figure 4 also shows that 17R4 has lower adsorbed mass than L64 at both temperatures. At the high concentration (18%, above *CMC*), adsorption of the copolymer occurs predominantly through the micelles [34,58]. L64 micelles have core-fringe structure [59] and 17R4 micelles have core-shell structure [60]. Core-fringe structure of L64 micelles allows PPO blocks to adsorb on the surface with low PEO blocks interference. Adversely, PEO shell in core-shell micelle of 17R4 prevents the adsorption as hydrophilic shell restricts the hydrophobic interaction between PPO core blocks and the surface. L64 unimers are also more hydrophobic than 17R4's. Thus, it is expected that L64 has higher adsorption (of both unimers and micelles) than 17R4 at both temperatures.

3.2. FTIR Molecular Analysis of the Film Residues on the Worn Surfaces and the Lubricants

FTIR is an infrared spectroscopy technique suited to detect the molecular structure of a sample. *FTIR* spectra of the *VO/W* emulsions and the aqueous copolymer solutions at 30 °C and 65 °C, and the residue films on the worn surfaces were obtained. Figure 5a shows the *FTIR* transmittance spectrum of worn surface lubricated with the 1% 10 kJ soybean *VO/W* emulsion at 65 °C and Figure 5b shows the spectrum of the emulsion. Similar spectra were obtained for both the ball and the disc for other lubricants. Figure 5a shows the transmittance spectrum of the worn track indicating the presence of alkane C–H bond (650–1000 cm^{-1} and 2900 cm^{-1}), ester C–O bond (1100 cm^{-1}), alkene C=C bond (1500 cm^{-1}), carboxylic acid C=O bond (1730 cm^{-1}), and water O–H bond (3610 cm^{-1}, 3730 cm^{-1}, and 3860 cm^{-1}). Variant peaks at wavenumber 2100–2350 cm^{-1} obtained on the surface are above 100% transmittance and are due to high noise of the solid surface. In Figure 5b spectrum, presence of alkane C–H bond (650–1000 cm^{-1}, 2810 cm^{-1} and 2900 cm^{-1}), ester C–O bond (1200 cm^{-1}), C=C double bond (1635 cm^{-1}), carboxylic acid C=O bond (1730 cm^{-1}), and water O–H bond (3330 cm^{-1}) within the emulsion are noted. Alkane C–H bond with different wavenumbers indicate the presence of hydrocarbon chain of fatty acid molecules while C=O and C–O bonds represent the presence of carboxylic acid functional groups and ester bonds between fatty acids and glycerol. The sharp peaks at 1500 cm^{-1} on the surface and 1635 cm^{-1} within the emulsion indicate the presence of the unsaturated C=C bond and the peaks at 3610–3860 cm^{-1} (sharp) on the surface and 3330 cm^{-1} (broad) within the emulsion are indicators of water molecules.
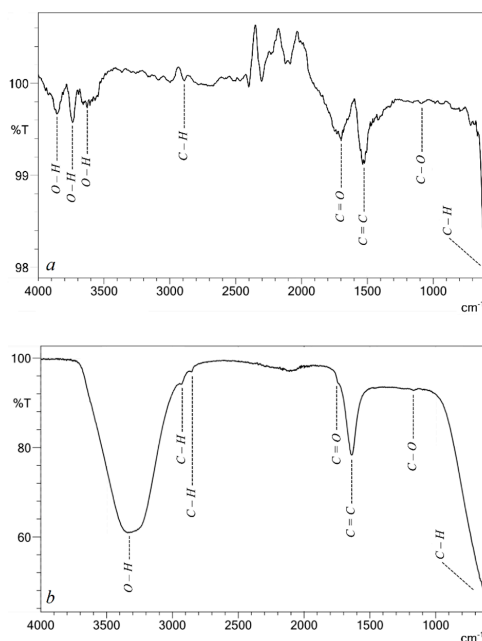

Figure 5. *FTIR* transmittance spectrum after the ball-on-disc test with 1% 10 kJ soybean *VO/W* emulsion at 65 °C (**a**) worn track and (**b**) the emulsion.

In Figure 5a,b, alkane C–H bonds within the aliphatic chain of both saturated and unsaturated fatty acids appear on the worn surface and the emulsion. C–O and C=O functional groups on worn track (Figure 5a) indicate the adsorption of soybean triglycerides to the surface through the polar glycerol head. C–O and C=O can also be indicative of the presence of primary oxidation product, ROOH hydroperoxide, from soybean oil oxidation in metal contact [25,29]. Alkene C=C bond at 1500 cm^{-1} is also an indication of the presence of unsaturated fatty acids (oleic, linoleic and linolenic) on the worn surfaces.

Tables 1 and 2 summarise the different peaks over the entire spectra range, showing similar elements and consequently the consistent presence of similar functional groups in each lubricating

group. As shown in Table 2, the main functional groups present in L64 and 17R4 copolymers solutions are alkane C–H, ester C–O, methylene CH_2, and alkyl CH_3 in a good agreement with the proposed structures shown in Figure 6a,b while the presence of alkane C–H, ester C–O, alkane C=C, and carboxylic acid C=O in soybean *VO/W* emulsion spectra is in agreement with fatty acid structures shown in Figure 6c–e. Both normal and reverse copolymers are non-ionic surfactants therefore expected to adsorb on SS316 surface predominantly through hydrophobic interactions of PPO blocks and surface [33]. In agreement with Figure 6a,b, analysis of the copolymer *FTIR* data of Table 2 indicates the presence of alkane C–H (specifically CH_2 and CH_3) and ester C–O groups within the copolymer solutions and on surface, but the presence of hydroxyl O–H groups only within the solutions. The presence of alkyl CH_3 bonds on surfaces coated with both copolymers, and the presence of hydroxyl O–H bond on surfaces coated with copolymer 17R4 only (Table 2 #16), confirms the adsorption of copolymers through the middle PPO and end PPO blocks in normal and reverse copolymers respectively [7,34]. In case of soybean *VO/W* emulsions, similar behaviour to 1% 10 kJ emulsion is observed for all emulsions indicating the adsorption of both saturated (stearic and palmitic acids) and unsaturated fatty acids with C=C double bonds (oleic, linoleic and linoleic) through the polar head of triglyceride.
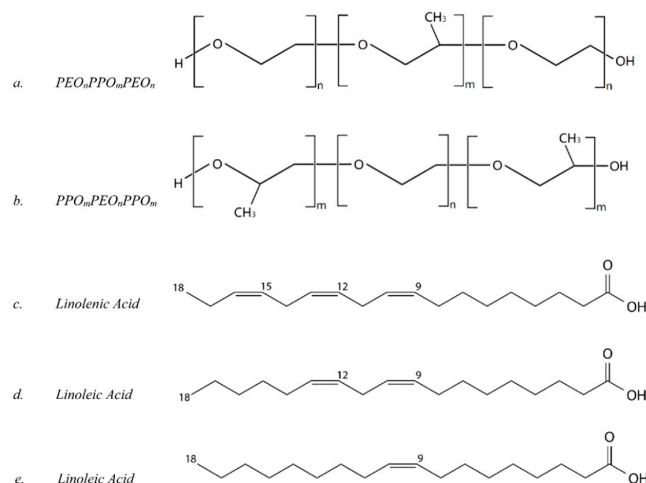
Figure 6. Schematic representations of copolymers molecules and unsaturated fatty acids within soybean oil.

Table 2. *FTIR* characterisation of solutions and worn surfaces (no temperature and concentration effect was noted).

| #	Peak Wavenumber (cm^{-1})	Element	Functional Group	Solution *	Surface **
1	650–1000	C–H	Alkanes	All	All
2	~1100	C–O	Ester	None	All
3	~1200	C–O	Ester	All	None
4	1350–1450	CH_2	Methylene	17R4 & L64	17R4 & L64 coated
5	1350–1450	CH_3	Alkyl	17R4 & L64	17R4 & L64 coated
6	~1500	C=C	Alkene	None	Soybean oil coated
7	~1635	C=C	Alkene	All	None
8	~1730	C=O	Carboxylic Acid	Soybean oil	Soybean oil coated
9	~2810	C–H	Alkanes	All	None
10	~2860	C–H	Alkanes	None	17R4 & L64 coated
11	~2900	C–H	Alkanes	All	All
12	~3330	O–H	-	All	None
13	~3610	O–H	-	None	Soybean oil coated
14	~3730	O–H	-	None	Soybean oil coated
15	~3860	O–H	-	None	Soybean oil coated
16	~3750	O–H	-	None	17R4 coated

* and ** after lubricity test.

3.3. Friction

The tribology performance of the two lubricants is assessed by measuring the friction and wear of the balls and the discs. Figure 7 shows the steady-state coefficient of friction of the 1% 10 kJ soybean *VO/W* emulsion obtained at 65 °C, in good agreement with the pure vegetable oil friction coefficient [15]. Figure 8 summarises the friction coefficients of all samples.
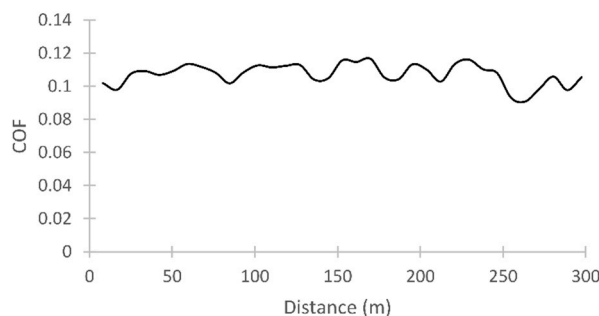
Figure 7. Friction coefficient trace of 1% 10 kJ soybean *VO/W* emulsion at 65 °C.
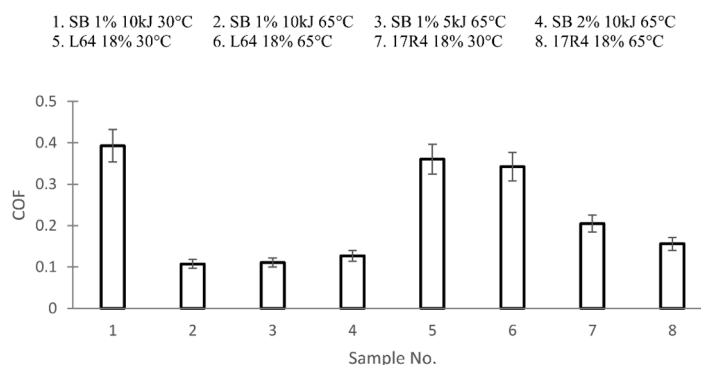
Figure 8. Friction coefficient average of all samples in 300 m sliding distance (SB indicates soybean emulsion).

From the comparison between soybean *VO/W* emulsions friction coefficients in Figure 8 (#1 to #4), it is seen that the friction coefficient of soybean *VO/W* emulsion is more sensitive to temperature than concentration and ultrasonication energy. At 30 °C, the friction coefficient is significantly higher (COF~0.39) compared to 65 °C (COF~0.11), indicating weaker adsorbed layer at 30 °C compared to 65 °C. With vegetable oil emulsions, the film formed on the sliding surface consist of both saturated and unsaturated fatty acids. Saturated fatty acids tend to align in a straight chain and populate the surface with a close-packed protection layer [14]. The *FTIR* data shown in Table 2 also indicate the presence of unsaturated fatty acids with C=C double bonds on the surface. In the boundary lubrication during the sliding contact between rubbing surfaces and due to high shear forces, bond cleavage between CH_2 segments of fatty acids may occur [25,49]. At 30 °C, the soybean droplets film on the surface is not strongly adhered through the polar bonds and cannot withstand the high shear force and the dynamic nature of the sliding test [49,52,53]. At 65 °C, soybean *VO/W* emulsions provide substantially better lubricity, primarily attributed to the induced chemical reactions of the adsorbed film with the surface oxide layer that triggers the surface chain polymerisation [48,49,53,61].

From Figure 8 (#2 and #4), it is noted that the concentration of soybean *VO/W* emulsion has slight adverse influence on friction reducing property at 65 °C. Figure 3c indicates a marginal increase in the adsorbed mass on the surface with increasing concentration from 1% to 2%. However, Figure 8 (#2 and #4) shows that friction coefficient increases from 0.11 to 0.13 with increasing concentration. It is known that due to the presence of a finite adsorption sites, there is a critical

surface concentration beyond which excess oil is unable to populate the surface due to the saturation of active adsorption sites. Beyond this concentration, the excess oil increases the intermolecular attraction forces (both hydrophobic and van der Waals attraction forces) between the adsorbed layer and the free oil droplets. This driving force results in weaker adsorbed film on surface. This agrees with previous studies where it is found that concentration only influences friction of vegetable oils in hexadecane only in concentrations below 1% [16,27].

Moreover, Figure 8 (#2 and #3) shows the adverse effect of ultrasonication energy on friction reducing property. Emulsification ultrasonic energy affects the oil droplet size. Larger droplets (5 kJ energy) have greater tendency to pre-adsorb on the surface (Figure 3a). However in ball-on-disc test, COF is seen to increase slightly from 0.10 to 0.11 by droplets size increase. This may be explained by considering the required adsorption dynamics in ball-on-disc test and slower rate of continuous readsorption of the larger droplets to the surface, resulting in an insignificant adsorption of larger droplets and therefore the negative influence of the droplet size on the friction coefficient.

According to Figure 8 (#5 to #8), the friction coefficient of copolymer aqueous solutions is higher compared to the soybean *VO/W* emulsions despite of the greater adsorbed mass of copolymers on surface (Figures 3 and 4). It is noted that the physically adsorbed layer is easily desorbed in the rinsing stage (Figure 4). This observation together with higher friction indicates the weaker films formed by L64 and 17R4 compared to the *VO/W* emulsions. The decreased adsorbed amount of copolymers with temperature increase was previously attributed to the dehydration and subsequently the shrinking of the PEO blocks. As the adsorbed layer properties influence the friction in boundary regime, this thin but dense film at high temperature withstands shear loads better, providing superior lubricity for copolymers at high temperature.

Comparing L64 and 17R4 solutions at 30 °C and 65 °C indicates the better lubricity of 17R4 solutions (Figure 8) albeit their lower adsorbed mass (Figure 4). Considering the amphiphilic nature of the copolymers, hydrophilic interaction between the PEO blocks of adsorbed layer and water in the bulk solution creates an adhesive hydrogen bond between the two [57]. Due to higher hydrophilic attraction force between the PEO blocks of the adsorbed film of 17R4 and water in the bulk solution compared to L64, lower COF of 17R4 compared to L64 is seen, contributed to the stronger affinity of 17R4 molecules to remain attached to both water and metal surface.

Regarding the effects of temperature on friction coefficient of copolymers, it should be noted that *QCM* measures the wet mass on the surface, i.e., the mass of the copolymer and the trapped water within the PEO blocks of the adsorbed copolymers. The shrinkage of the PEO blocks in high temperature corresponds to the removal of the trapped water within the block chain. This removal of water from PEO blocks however does not influence the hydrophilic attraction forces between the PEO blocks of the adsorbed film and water in the bulk solution. Therefore, while more hydrophobic L64 copolymer represents higher adsorbed mass than 17R4 on surface (more so at high temperature), but linkage between metal surface and water through the adsorption of 17R4 to metal surface results in more barriers against the shear force, therefore reduces the friction to higher extent. Moreover, the density of the film between friction pairs also increases with increasing temperature due to the removal of the trapped coupled water molecules from the PEO blocks of adsorbed film. Therefore, increased density of the film also reduces the friction coefficient for the copolymer solutions at high temperature.

3.4. Worn Track and Ball Scar Analysis

In metal forming, metal to metal contact results in wear and abrasion where the severity depends on the strength of the adsorbed film between the rubbing pairs. Figure 9 shows the morphological *SEM* images of worn balls surfaces lubricated with soybean *VO/W* emulsions. A large elliptic wear scar is seen on the ball lubricated with 1% 10 kJ soybean *VO/W* emulsion at 30 °C (Figure 9a), but is hardly seen on the ball lubricated with the same emulsion at 65 °C (Figure 9b) even though scar tracks are still notifiable on the respective disc (Figure 10). Similar results are obtained for other soybean *VO/W* emulsions at 65 °C (Figure 9c,d) showing the tenacious film residues left on the balls surfaces

lubricated at 65 °C. It is also noted that the scar diameters of the 30 °C *VO/W* emulsion are comparable to those lubricated by the aqueous copolymer solutions (Figure 11). Negligible wear scar on balls lubricated with vegetable oils in high temperature has also been identified by Knothe [62] in case of oleic and linoleic acid based lubricants at 60 °C. Table 3 summarizes the wear quantities for all lubricants. Low friction of 65 °C soybean *VO/W* emulsions is in agreement with almost non-visible wear scar on the ball and small disc wear track width. However, at low temperature (30 °C) soybean *VO/W* emulsion does not provide sufficient protective layer resulting in the wear scar width of 0.85 mm, COF of 0.393 and the removal of 0.15 µg wear debris. In this case, wear scar is clearly seen on the ball (Figure 9a) with an area of 0.68 mm^2.

Figure 10 shows the worn surfaces of the balls and discs lubricated by 1% 10 kJ soybean *VO/W* emulsions at 30 °C and 65 °C. At 30 °C, worn surfaces on the ball (Figure 9a) and the disc (Figure 10a) have similar topographical features indicating severe surface-to-surface contacts and high friction coefficient (COF: 0.39, Figure 8 #1). In contrast with 65 °C emulsion, worn scar is not visible on the ball (Figure 9b) while worn track is visible on the disc (Figure 10b). This behaviour confirms Kenbeck and Bunemann [48] hypothesis postulating the low surface activity of soybean *VO/W* droplets at low temperature. 1% 5 kJ and 2% 10 kJ soybean *VO/W* emulsions show similar behaviour to 1% 10 kJ emulsion, indicating the dominant effects of temperature and negligible effects of increasing the input energy and concentration on the lubricity of *VO/W* emulsions.
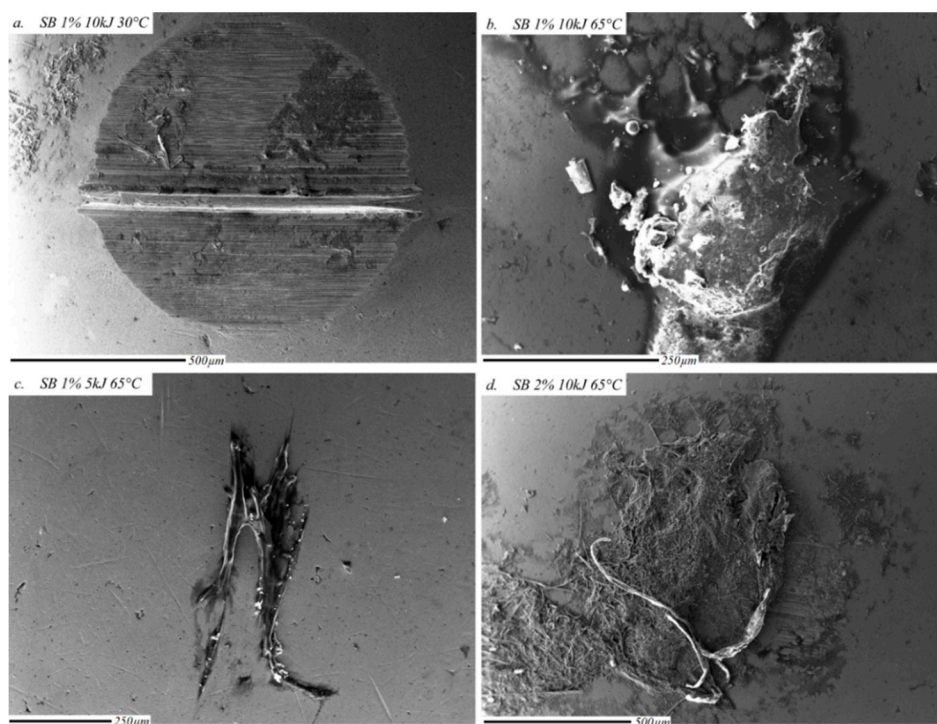
Figure 9. Morphological *SEM* images of wear scar on balls after friction test on soybean *VO/W* emulsions.

Table 3. Discs and balls scar dimensions.

#	Concentration (%)	Preparation Energy (kJ)	T (°C)	Disc Scar Width (mm)	Ball Scar Area (mm^2)	Ball Mass Loss (µg)	COF
L64	18	N/A	30	0.89	0.87	0.24	0.360
L64	18	N/A	65	1.23	1.69	0.94	0.342
17R4	18	N/A	30	0.88	0.60	0.11	0.205
17R4	18	N/A	65	1.15	1.21	0.47	0.156
Soybean	1	10	30	0.85	0.68	0.15	0.393
Soybean	1	10	65	0.34	Non Visible	Non Visible	0.107
Soybean	1	5	65	0.35	Non Visible	Non Visible	0.110
Soybean	2	10	65	0.39	Non Visible	Non Visible	0.127
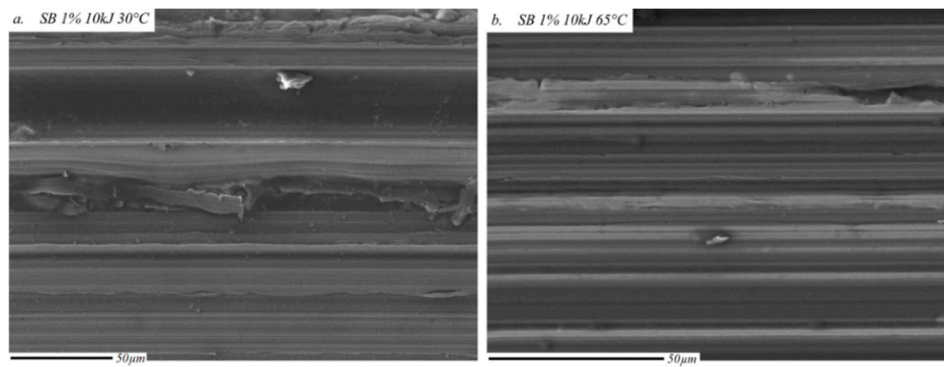
Figure 10. Morphological *SEM* images of scar tracks on discs after lubricity test on 1% 10 kJ soybean *VO/W* emulsions.

Figure 11 shows the morphological *SEM* images of the worn balls and Figure 12 shows the wear track on the discs lubricated by copolymer solutions. Both the balls scar diameters and the discs worn track widths (Table 3) of the 17R4 solutions are smaller than the L64 solutions at both temperatures. This correlates with the lower COF for the 17R4 compared to the L64 at both temperatures. However, the effect of temperature on COF and wear seems contradictory. As shown in Table 3, although the lubricity of both copolymer solutions is improved at high temperature, but increased wear is also observed on both discs and balls at higher temperature.
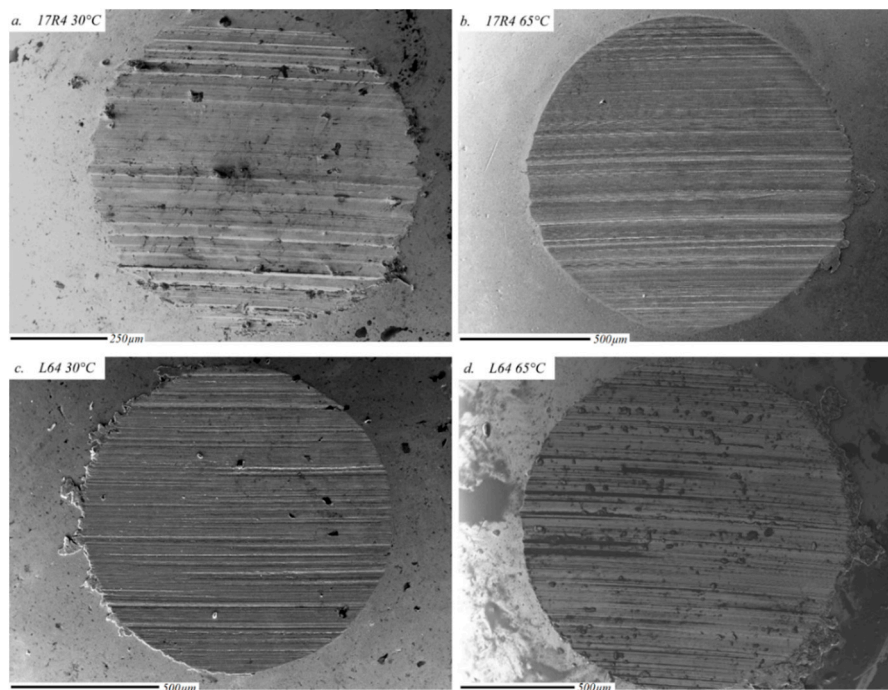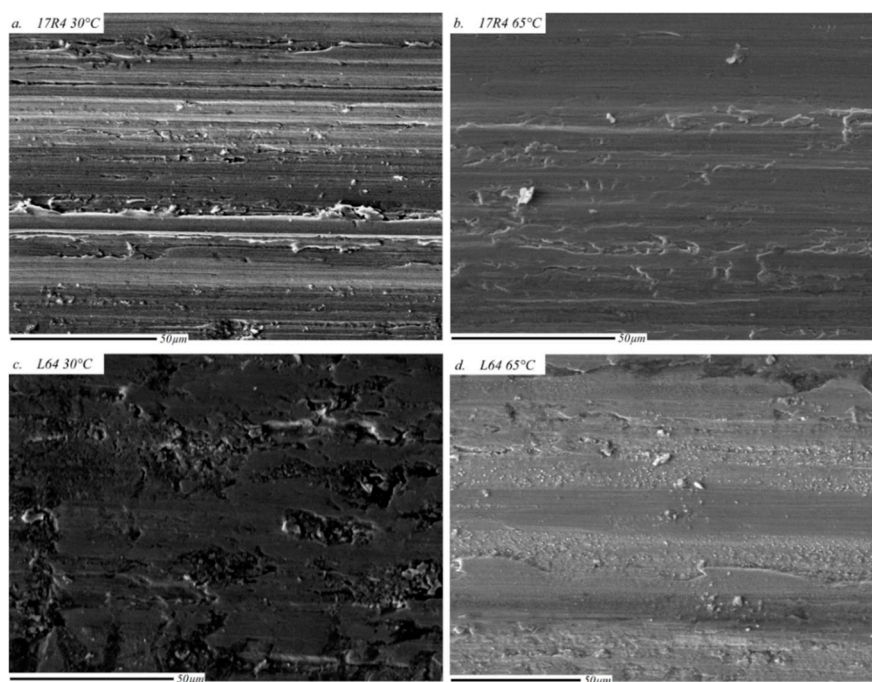

Figure 11. Morphological *SEM* images of wear scar on balls after friction test on copolymer solutions.

At 65 °C, hydrophobicity of both copolymers increases. This transition not only creates higher copolymer-surface affinity through the PPO blocks, but also results in a dense dehydrated film on the surface. This thin and dense layer between the rubbing pairs, decreases the scar depth and the COF, but results in increased contact area and therefore the scar width/area on the discs/balls. Figures 11a and 12a show the deep grooves of 30 °C wear track for 17R4 solution indicating the dominant ploughing wear mechanism compared to 65 °C (Figures 11b and 12b). This explains the

lower COF at 65 °C for 17R4 solution despite of larger scar dimensions. Figures 11 and 12 also show a similar behaviour with L64 solutions at the two temperatures where ploughing wear result in deep groove at 30 °C (Figures 11c and 12c) compared to significantly shallower groove with plastic deformation wear at 65 °C (Figures 11d and 12d). The lower friction of higher temperature is assigned to the adhesion friction (plastic deformation) while at lower temperature ploughing and abrasion friction is dominant. At low temperature when water in trapped within the PEO blocks of copolymers, sliding force can easily shred the lubricating film on the surface and result in higher friction and direct contacts with deep but narrow width wear area. Higher density of the lubricating film in high temperature have higher tendency to spread the sliding force. Therefore, higher area between lubricating pairs is affected by the sliding force, indicating shallower, but larger wear area in high temperature, with low friction coefficient.

Figure 12. Morphological *SEM* images of scar tracks on discs after lubricity test on copolymer solutions.

3.5. Surface Cleanliness

Figure 13 shows the optical images of disc surfaces after the ball-on-disc tests. The discs were ultrasonically cleaned with acetone for 20 min and then rinsed with *Milli-Q* water. It is clearly demonstrated that the adsorbed copolymer layer can be removed from the surface by means of a simple surface cleaning process (Figure 13 left) while those lubricated by the *VO/W* emulsions still have residue on the surface (Figure 13 right). While vegetable oils tendency to produce ROOH hydroperoxide through oxidation results in thickening, varnish formation and sludge deposition on surfaces [26,63] and postulates poor cleanability, triblock copolymers have high wetting and spreading ability, thus are easily rinsed with *Milli-Q* water [8,20]. This direct observation, together with the *QCM* film removal of Figures 3 and 4 at rinsing stage (above 20 min) demonstrates the superior surface cleanability of the copolymer solutions compared to the *VO/W* emulsions, albeit with higher friction and wear.
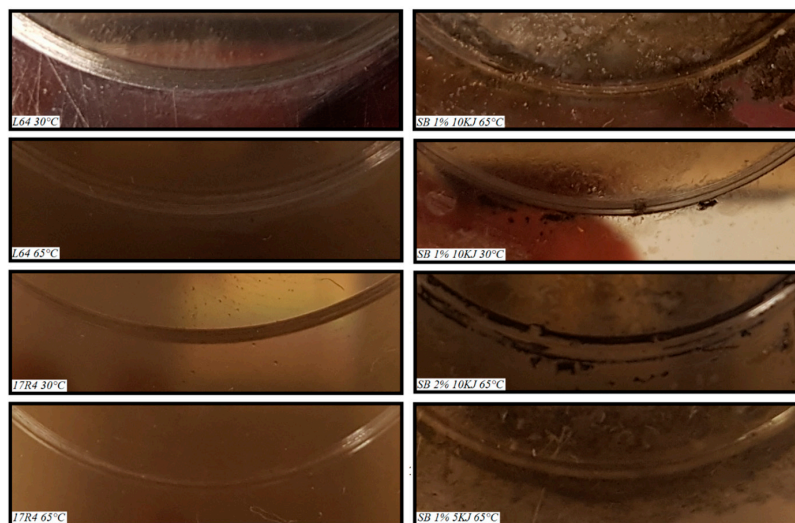
Figure 13. Optical images of discs surfaces after 20 min ultrasonic cleaning.

4. Conclusions

Surface film adsorption and lubricity of the two different types of environmentally friendly lubricants namely soybean *VO/W* emulsions and triblock copolymer solutions were investigated.

The results showed that the adsorption of soybean oil droplets increases with temperature and concentration, more so with temperature. Increasing input energy from 5 kJ to 10 kJ decreased the adsorbed mass of droplets, attributed to the reduced droplets size. For the aqueous copolymer solutions, temperature was seen to adversely affect the copolymer adsorption, more so for 17R4 solution than L64.

Infrared spectroscopy on the worn surfaces indicated the presence of both saturated and unsaturated fatty acids of soybean oil and the enhanced lubricity with temperature was attributed to the increased surface affinity of the unsaturated fatty acids and formation of chemical layers on surface at high temperature. It was also postulated that the triblock copolymers are attracted to the metal surface through hydrophobic PPO blocks via hydrophobic forces, regardless of the blocks positioning within the structure. The nature of the film formation and the attraction forces between films and surface was seen to affect the cleanability of the two water based lubricants.

Overall, the substitution of the mineral oil emulsions with environmentally-friendly water-based alternatives was investigated, indicating the reduced friction and wear, more for *VO/W* emulsions, but superior surface cleanliness for copolymer solutions indicating the reduced post-process brushing and cleaning operations (e.g., smooth cleaning, degreasing etc.) for copolymer solutions compared to *VO/W* emulsions, favourable in many metal forming applications.

Author Contributions: Reza Taheri and Buyung Kosasih conceived and designed the experiments; Reza Taheri performed the experiments; Reza Taheri and Buyung Kosasih analysed the data; Hongtao Zhu and Anh Kiet Tieu contributed reagents/materials/analysis tools; Reza Taheri, Buyung Kosasih, Hongtao Zhu and Anh Kiet Tieu wrote the paper.

Conflicts of Interest: The authors declare no conflict of interest.

References

1. Menezes, P.L.; Reeves, C.J.; Lovell, M.R. Fundamentals of lubrication. In *Tribology for Scientists and Engineers*; Menezes, P.L., Ingole, S.P., Nosonovsky, M., Kailas, S.V., Lovell, M.R., Eds.; Springer: New York, USA, 2013; pp. 295–296.

2. Cambiella, A.; Benito, J.M.; Pazos, C.; Coca, J.; Ratoi, M.; Spikes, H.A. The effect of emulsifier concentration on the lubricating properties of oil-in-water emulsions. *Tribol. Lett.* **2006**, *22*, 53–65. [CrossRef]

3. Tieu, A.K.; Kosasih, P.B.; Godbole, A. A thermal analysis of strip-rolling in mixed-film lubrication with o/w emulsions. *Tribol. Int.* **2006**, *39*, 1591–1600. [CrossRef]

4. Tieu, A.K.; Kosasih, P.B. Experimental and numerical study of o/w emulsion lubricated strip rolling in mixed film regime. *Tribol. Lett.* **2007**, *25*, 23–32. [CrossRef]

5. Wang, A.; Chen, L.; Jiang, D.; Zeng, H.; Yan, Z. Vegetable oil-based ionic liquid microemulsion biolubricants: Effect of integrated surfactants. *Ind. Crops Prod.* **2014**, *62*, 515–521. [CrossRef]

6. Jain, A.; Bisht, R.P.S. Metalworking emulsions from industrial vegetable oils. *J. Synth. Lubr.* **2008**, *25*, 87–94. [CrossRef]

7. Kosasih, B.; Novareza, O.; Tieu, K.; Zhu, H. Friction and anti-wear property of aqueous tri-block copolymer solutions in metal forming. *Int. J. Surf. Sci. Eng.* **2014**, *8*, 109–123. [CrossRef]

8. Kosasih, B.; Novareza, O.; Zhu, H.; Taheri, R.; Lin, B.; Tieu, A.K. Thickness and scratch resistance of adsorbed film formed by triblock symmetrical copolymer solutions. *Lubr. Sci.* **2016**, *28*, 299–315. [CrossRef]

9. Lee, S.; Spencer, N.D. Poly(L-lysine)-graft-poly(ethylene glycol): A versatile aqueous lubricant additive for tribosystems involving thermoplastics. *Lubr. Sci.* **2008**, *20*, 21–34. [CrossRef]

10. Alexandridis, P.; Hatton, T.A. Poly(ethylene oxide)-poly(propylene oxide)-poly(ethylene oxide) block copolymer surfactants in aqueous solutions and at interfaces: Thermodynamics, structure, dynamics, and modeling. *Colloids Surf. A Physicochem. Eng. Asp.* **1995**, *96*, 1–46. [CrossRef]

11. Pfister, D.P.; Xia, Y.; Larock, R.C. Recent advances in vegetable oil-based polyurethanes. *ChemSusChem* **2011**, *4*, 703–717. [CrossRef] [PubMed]

12. Odi-Owei, S. Tribological properties of some vegetable oils and fats. *Lubr. Eng.* **1998**, *45*, 685–690.

13. Joseph, P.V.; Sharma, D.K. Improvement of thermooxidative stability of non-edible vegetable oils of indian origin for biodegradable lubricant application. *Lubr. Sci.* **2010**, *22*, 149–161. [CrossRef]

14. Siniawski, M.T.; Saniei, N.; Adhikari, B.; Doezema, L.A. Influence of fatty acid composition on the tribological performance of two vegetable-based lubricants. *J. Synth. Lubr.* **2007**, *24*, 101–110. [CrossRef]

15. Joseph, P.V.; Saxena, D.; Sharma, D.K. Study of some non-edible vegetable oils of indian origin for lubricant application. *J. Synth. Lubr.* **2007**, *24*, 181–197. [CrossRef]

16. Biresaw, G.; Adhvaryu, A.; Erhan, S.Z. Friction properties of vegetable oils. *J. Am. Oil Chem. Soc.* **2003**, *80*, 698–704. [CrossRef]

17. Quinchia, L.A.; Delgado, M.A.; Reddyhoff, T.; Gallegos, C.; Spikes, H.A. Tribological studies of potential vegetable oil-based lubricants containing environmentally friendly viscosity modifiers. *Tribol. Int.* **2014**, *69*, 110–117. [CrossRef]

18. Padmini, R.; Krishna, P.V.; Rao, G.K.M. Effectiveness of vegetable oil based nanofluids as potential cutting fluids in turning aisi 1040 steel. *Tribol. Int.* **2016**, *94*, 490–501. [CrossRef]

19. Burton, G.; Goo, C.-S.; Zhang, Y.; Jun, M.B.G. Use of vegetable oil in water emulsion achieved through ultrasonic atomization as cutting fluids in micro-milling. *J. Manuf. Process.* **2014**, *16*, 405–413. [CrossRef]

20. Li, Y.; Rojas, O.J.; Hinestroza, J.P. Boundary lubrication of peo-ppo-peo triblock copolymer physisorbed on polypropylene, polyethylene, and cellulose surfaces. *Ind. Eng. Chem. Res.* **2012**, *51*, 2931–2940. [CrossRef]

21. Zhang, C.; Liu, J.; Zhang, C.; Liu, S. Friction reducing and anti-wear property of metallic friction pairs under lubrication of aqueous solutions with polyether added. *Wear* **2012**, *292–293*, 11–16. [CrossRef]

22. Nakahara, T.; Makino, T.; Kyogoku, K. Observations of liquid droplet behavior and oil film formation in o/w type emulsion lubrication. *J. Tribol.* **1988**, *110*, 348–353. [CrossRef]

23. Nakanishi, H.; Saiki, K.; Hirayama, T.; Matsuoka, T. Variation of oil introduction behaviour during oil-in-water emulsion rolling. *Mater. Trans.* **2013**, *54*, 1408–1415. [CrossRef]

24. Barker, D.C.; Johnstona, G.J.; Spikesa, H.A.; Bunemannb, T.F. Ehd film formation and starvation of oil-in-water emulsions. *Tribol. Trans.* **1993**, *36*, 565–572. [CrossRef]

25. Fox, N.J.; Stachowiak, G.W. Boundary lubrication properties of oxidized sunflower oil. *J. Soc. Tribol. Lubr. Eng.* **2003**, *59*, 15–20.

26. Boyde, S. Green lubricants. Environmental benefits and impacts of lubrication. *Green Chem.* **2002**, *4*, 293–307. [CrossRef]

27. Adhvaryu, A.; Erhan, S.Z.; Perez, J.M. Tribological studies of thermally and chemically modified vegetable oils for use as environmentally friendly lubricants. *Wear* **2004**, *257*, 359–367. [CrossRef]

28. Biresaw, G. Adsorption of amphiphiles at an oil–water vs. An oil–metal interface. *J. Am. Oil Chem. Soc.* **2005**, *82*, 285–292. [CrossRef]

29. Das, L.M.; Bora, D.K.; Pradhan, S.; Naik, M.K.; Naik, S.N. Long-term storage stability of biodiesel produced from karanja oil. *Fuel* **2009**, *88*, 2315–2318. [CrossRef]

30. D'Errico, G.; Paduano, L.; Khan, A. Temperature and concentration effects on supramolecular aggregation and phase behavior for poly(propylene oxide)-b-poly(ethylene oxide)-b-poly(propylene oxide) copolymers of different composition in aqueous mixtures, 1. *J. Colloid Interface Sci.* **2004**, *279*, 379–390. [CrossRef] [PubMed]

31. Alexandridis, P. Poly(ethylene oxide)/poly(propylene oxide) block copolymer surfactants. *Curr. Opin. Colloid Interface Sci.* **1997**, *2*, 478–489. [CrossRef]

32. Kiss, É.; Erdélyi, K.; Szendrö, I.; Vargha-Butler, E.I. Adsorption and wetting properties of pluronic block copolymers on hydrophobic surfaces studied by optical waveguide lightmode spectroscopy and dynamic tensiometric method. *J. Adhes.* **2004**, *80*, 815–829. [CrossRef]

33. Novareza, O. Tribology of aqueous Copolymer Lubricants for Metal Forming Applications. Ph.D. Thesis, University of Wollongong, Wollongong, Australia, 2014.

34. Taheri, R.; Kosasih, B.; Zhu, H.; Tieu, A.K. Phase behaviour and lubricity of aqueous PEO-PPO-PEO and ppo-peo-ppo triblock copolymer solutions. *Tribol. Trans.* **2016**, 1–9. [CrossRef]

35. Shar, J.A.; Obey, T.M.; Cosgrove, T. Adsorption studies of polyethers part ii: Adsorption onto hydrophilic surfaces. *Colloids Surf. A Physicochem. Eng. Asp.* **1999**, *150*, 15–23. [CrossRef]

36. Shar, J.A.; Obey, T.M.; Cosgrove, T. Adsorption studies of polyethers part i. Adsorption onto hydrophobic surfaces. *Colloids Surf. A Physicochem. Eng. Asp.* **1998**, *136*, 21–33. [CrossRef]

37. Lee, S.; Iten, R.; Muller, M.; Spencer, N.D. Influence of molecular architecture on the adsorption of poly(ethylene oxide)-poly(propylene oxide)-poly(ethylene oxide) on pdms surfaces and implications for aqueous lubrication. *Macromolecules* **2004**, *37*, 8349–8356. [CrossRef]

38. Brandani, P.; Stroeve, P. Adsorption and desorption of PEO-PPO-PEO triblock copolymers on a self-assembled hydrophobic surface. *Macromolecules* **2003**, *36*, 9492–9501. [CrossRef]

39. Dibble, K. Chemical Cleaning of Metals. Available online: http://nzic.org.nz/ChemProcesses/metals/8H.pdf (accessed on 15 December 2016).

40. Liu, K. *Soybeans: Chemistry, Technology and Utilization*; Chapman & Hall: New York, NY, USA, 1997.

41. Martin, S.J.; Granstaff, V.E.; Frye, G.C. Characterization of a quartz crystal microbalance with simultaneous mass and liquid loading. *Anal. Chem.* **1991**, *63*, 2272–2281. [CrossRef]

42. Kanazawa, K.K.; Gordon, J.G.I. The oscillation frequency of a quartz resonator in contact with a liquid. *Anal. Chim. Acta* **1985**, *175*, 99–105. [CrossRef]

43. Lynn, J.L.J. Detergents and detergency. In *Bailey's Industrial Oil and Fat Products*, 6th ed.; Shahidi, F., Ed.; John Wiley & Sons: Hoboken, NJ, USA, 2005; pp. 164–166.

44. Stalgren, J.J.R.; Claesson, P.M.; Warnheim, T. Adsorption of liposomes and emulsions studied with a quartz crystal microbalance. *Adv. Colloid Interface Sci.* **2001**, *89–90*, 383–394. [CrossRef]

45. Abismail, B.; Canselier, J.P.; Wilhelm, A.M.; Delmas, H.; Gourdon, C. Emulsification by ultrasound: Drop size distribution and stability. *Ultrason. Sonochem.* **1999**, *6*, 75–83. [CrossRef]

46. Atkins, P.; de Paula, J. *Physical Chemistry*, 8th ed.; W. H. Freeman and Company: New York, NY, USA, 2006.

47. Connell, S.D.A.; Allen, S.; Roberts, C.J.; Davies, J.; Davies, M.C.; Tendler, S.J.B.; Williams, P.M. Investigating the interfacial properties of single-liquid nanodroplets by atomic force microscopy. *Langmuir* **2002**, *19*, 1719–1728. [CrossRef]

48. Kenbeck, D.; Bunemann, T.F. Organic friction modifiers. In *Lubricant Additives: Chemistry and Applications*, 2nd ed.; Rudnick, L.R., Ed.; CRC Press: New York, NY, 2009; pp. 201–202.

49. Adhvaryu, A.; Erhan, S.Z. Epoxidized soybean oil as a potential source of high-temperature lubricants. *Ind. Crops Prod.* **2002**, *15*, 247–254. [CrossRef]

50. Beltzer, M.; Jahanmir, S. Effect of additive molecular structure on friction. *Lubr. Sci.* **1988**, *1*, 3–26. [CrossRef]

51. Jahanmir, S.; Beltzer, M. Effect of additive molecular structure on friction coefficient and adsorption. *J. Tribol.* **1986**, *108*, 109–116. [CrossRef]

52. Rossrucker, T.; Fessenbecker, A. Sulfur carriers. In *Lubricant Additives: Chemistry and Applications*, 2nd ed.; Rudnick, L.R., Ed.; CRC Press: New York, NY, USA, 2009; pp. 267–269.

53. Phillips, W.D. Ashless phosphorus-containing lubricating oil additives. In *Lubricant Additives: Chemistry and Applications*, 2nd ed.; Heinemann, H., Ed.; CRC Press: New York, NY, USA, 2009; pp. 78–79.

54. Liu, X.; Wu, D.; Turgman-Cohen, S.; Genzer, J.; Theyson, T.W.; Rojas, O.J. Adsorption of a nonionic symmetric triblock copolymer on surfaces with different hydrophobicity. *Langmuir* **2010**, *26*, 9565–9574. [CrossRef] [PubMed]

55. Viitala, T.; Liang, H.; Gupta, M.; Zwinger, T.; Yliperttula, M.; Bunker, A. Fluid dynamics modeling for synchronizing surface plasmon resonance and quartz crystal microbalance as tools for biomolecular and targeted drug delivery studies. *J. Colloid Interface Sci.* **2012**, *378*, 251–259. [CrossRef] [PubMed]

56. Caragheorgheopol, A.; Schlick, S. Hydration in the various phases of the triblock copolymers $eo_{13} po_{30} eo_{13}$ (pluronic l64) and $eo_6 po_{34} eo_6$ (pluronic l62), based on electron spin resonance spectra of cationic spin probes. *Macromolecules* **1998**, *31*, 7736–7745. [CrossRef]

57. Cohn, D.; Lando, G.; Sosnik, A.; Garty, S.; Levi, A. PEO-PPO-PEO-based poly(ether ester urethane)s as degradable reverse thermo-responsive multiblock copolymers. *Biomaterials* **2006**, *27*, 1718–1727. [CrossRef] [PubMed]

58. Green, R.J.; Tasker, S.; Davies, J.; Davies, M.C.; Roberts, C.J.; Tendler, S.J.B. Adsorption of PEO-PPO-PEO triblock copolymers at the solid/liquid interface: A surface plasmon resonance study. *Langmuir* **1997**, *13*, 6510–6515. [CrossRef]

59. Patel, T.; Bahadur, P.; Mata, J. The clouding behaviour of PEO-PPO based triblock copolymers in aqueous ionic surfactant solutions: A new approach for cloud point measurements. *J. Colloid Interface Sci.* **2010**, *345*, 346–350. [CrossRef] [PubMed]

60. Li, Y.; Liu, H.; Song, J.; Rojas, O.J.; Hinestroza, J.P. Adsorption and association of a symmetric PEO-PPO-PEO triblock copolymer on polypropylene, polyethylene, and cellulose surfaces. *ACS Appl. Mater. Interfaces* **2011**, *3*, 2349–2357. [CrossRef] [PubMed]

61. Murakami, T.; Sakamoto, H. Lubricating properties of vegetable oils and paraffinic oils with unsaturated fatty acids under high-contact-pressure conditions in four-ball tests. *J. Synth. Lubr.* **2003**, *20*, 183–201. [CrossRef]

62. Knothe, G. Evaluation of ball and disc wear scar data in the hfrr lubricity test. *Lubr. Sci.* **2008**, *20*, 35–45. [CrossRef]

63. Pantoja, S.S.; da Conceição, L.R.V.; da Costa, C.E.F.; Zamian, J.R.; da Rocha Filho, G.N. Oxidative stability of biodiesels produced from vegetable oils having different degrees of unsaturation. *Energy Convers. Manag.* **2013**, *74*, 293–298. [CrossRef]